

Characterizations of Interfacial Heat Transfer for Electronic Packages by Multiscale Modeling

Ningbo Liao and Ping Yang*

Jiangsu University, 212013 Zhenjiang, People's Republic of China

DOI: 10.2514/1.35419

Thermal design of electronic packages is an important topic in electronic manufacturing. Interfaces of dissimilar materials in electronic packages are prone to crack initiations, leading to delaminations. Many of the predecessors' works are based on overall simulations. But with one model to cover the entire package, the resolution of thermal states near the interface is limited. In this paper, a multiscale model is proposed for interfacial thermal conductance of dissimilar materials. In this coupled model, the continuum subdomain is used as a boundary model that provides the low-frequency impedance and a sink for the energy associated with outgoing waves of the molecular dynamics model. The boundary conditions can be applied to the finite element model more easily. The simulation results show that the temperature distribution is nonuniform along the interface, with several places corresponding to a large temperature difference and severe plastic deformation. In the meantime, the copper–copper interface is investigated as an example. The corresponding vector-field results of atom displacements and the temperature distribution are presented. The results show that the characteristic of atoms moving along the interface is caused by a dissimilarity of material, which reveals the damage mechanism at the interface in heat transfer, and so the method can be used to investigate other interfacial behaviors of dissimilar materials.

Nomenclature

C_p	=	constant pressure specific heat
E_j	=	kinetic energy of all atoms in the sphere
$F_i(\rho_i)$	=	embedding energy of atom i with electron density ρ_i .
H	=	quadrature weight associated with point X_n
h	=	heat transfer coefficient
I	=	element.
K_{iajb}	=	integral in the definition of the stiffness matrix
k	=	thermal conductivity
k_B	=	Boltzmann constant
M_{IJ}	=	components of finite element mass matrix
m	=	mass
N_a	=	number of atoms
N_c	=	number of nodes in the finite element region
n	=	outward surface normal
Q	=	volumetric heat source
\dot{q}	=	atomic velocity
q_0	=	displacement at the atomistic/continuum interface
r_{ij}	=	separation distance between atoms i and j
T	=	temperature at the interface
T_{inf}	=	temperature of the surrounding environment
t	=	time
Γ	=	transmission coefficient of the material of origin for the mode of propagation
θ	=	angle of incidence
ρ_i	=	electron density
ρ	=	material density
$\phi_{ij}(r_{ij})$	=	two-body central potential between atoms i and j with the separation distance r_{ij}
Ω_I	=	volume

I. Introduction

ELECTRONIC packages usually consist of bonded materials with different thermal and mechanical properties. Thermal loading during various stages of the fabrication, assembly, and qualification will induce high stresses in the electronic package. The delamination of interfaces may occur because of high stresses. Some literature discusses the various interfaces with different methods [1–22]. A number of approaches have been developed to investigate interfacial delamination. It is generally accepted that the propagation of interfacial delamination can be evaluated by the fracture failure criteria. However, the extent, location, and size of the delamination or the crack cannot be easily determined in real packages; it thus poses a problem for predicting failure at interfaces in integrated circuit packages. Thermal stress in a metal system is most often studied with the finite element method (FEM), which lies, in part, on the continuum theory of elasticity. However, when the system becomes extremely small, the atomistic effects have to be taken into account correctly. The conventional FEM is not capable of accurately capturing all of the information, especially when applying it to the small dimensions. Ye et al. [1] reviewed the failure modes of insulated gate bipolar transistors and presented a FEM analysis of a multilayered insulated gate bipolar transistor packaging module under cyclic thermal loading. The results showed that the thermal cycling has a significant effect on the solder-layer reliability. A natural approach to the simulation of multiscale processes is thus to combine an atomic simulation for the critical regions within the system with a continuum method for the remainder of the system. Ji and Gao [2] discussed fracture mechanisms in biological nanocomposites. In this paper, the virtual internal bond model has been developed to investigate failures in bimaterial systems on both macro- and microlevels. The virtual internal bond model is a continuum mechanics method with a built-in phenomenological atomic interaction potential. The constitutive law in the model is a hyperelastic stress–strain law derived from the average property of a virtual network of atomic bonds. Fan et al. [3] discussed a new method to predict delamination in electronic packages. A model was built to determine the interfacial energy between epoxy molding compound and copper substrate by combining experimental data. The interfacial material properties were evaluated by considering the interaction energy between epoxy molding compound and Cu substrate. The force-distance curve obtained directly by atomic force microscopy is used to determine the interfacial material properties. The properties were used in the multiscale model.

Received 12 November 2007; revision received 21 May 2008; accepted for publication 7 June 2008. Copyright © 2008 by the American Institute of Aeronautics and Astronautics, Inc. All rights reserved. Copies of this paper may be made for personal or internal use, on condition that the copier pay the \$10.00 per-copy fee to the Copyright Clearance Center, Inc., 222 Rosewood Drive, Danvers, MA 01923; include the code 0887-8722/08 \$10.00 in correspondence with the CCC.

*Professor, Laboratory of Materials and Micro-Structural Integrity, School of Mechanical Engineering; yangpingdm@ujs.edu.cn.

At the microscopic length scale, the molecular dynamics (MD) method correctly takes into account these effects when the potential is chosen correctly. In this paper, a novel hybrid MD/finite element (FE) simulation approach is proposed to investigate the characteristics at the interface of dissimilar materials during the heat transport process. An atomic model is coupled with the finite element model at the boundaries of atoms, so that boundary conditions could be applied more readily to the model. There are few direct experimental measurements of heat transfer through interface, because it is very costly and the effects of such variables as temperature near the interface, material properties, etc., are very hard to measure experimentally. However, similar experimental results support the conclusions in this paper.

II. Computational Methodology

In this paper, the embedded-atom method is used to describe the interatomic interactions between Al–Al, Cu–Cu, and Al–Cu. The embedded-atom method has been widely used to describe the mechanical behavior of pure metals and alloys. Nowadays, it is probably the most popular method to simulate mechanical properties of metals at the atomic level [4–9]. The embedded-atom method defines the energy E of the system as the sum of energies for each atom i , with each atom having energy contributions from an embedding function F that depends on a local electron density and a pair potential, so that

$$E = \sum_i F_i(\rho_i) + \frac{1}{2} \sum_{i \neq j} \phi_{ij}(r_{ij}) \quad (1)$$

where $\phi_{ij}(r_{ij})$ is a two-body central potential between atoms i and j with the separation distance r_{ij} , and $F_i(\rho_i)$ is the embedding energy of atom i with the electron density ρ_i . For the binary system, the pair potential function of dissimilar materials $\phi_{ab}(r)$ is important to describe the interfacial interactivities of atoms. In this paper, Johnson's alloy model [5] is used to describe the interatomic potentials. The function $\phi_{ab}(r)$ is summed to be a density-weighted combination of monoatomic parallel to the interfaces. It can be defined as follows:

$$\phi_{ab}(r) = \frac{1}{2} \left[\frac{f_b(r)}{f_a(r)} \phi_a(r) + \frac{f_a(r)}{f_b(r)} \phi_b(r) \right] \quad (2)$$

where a and b represent the two different materials.

The finite element modeling expression for the potential energy can be yielded as follows [8]:

$$U^{\text{FE}} = \sum_I U_I^{\text{FE}} \quad (3)$$

$$U_I^{\text{FE}} = \frac{1}{2} K_{iajb;l} u_{ia} u_{jb} \quad (4)$$

$$K_{iajb;l} = C_{acbd} \int_{\Omega_l} d^3x \partial_c N_i(x) \partial_d N_j(x) \quad (5)$$

where the integral in the definition of the stiffness matrix K_{iajb} is over the volume Ω_l of element l . This integral can be calculated analytically or numerically in some cases. The stiffness matrix is assembled element by element for efficiency, so that there is a global stiffness matrix given by [8]

$$K_{iajb} = \sum_l K_{iajb;l}$$

III. Calculating Method for Thermal Parameters in MD

The instantaneous temperature of each site at a certain time step is taken as the mean temperature over a neighborhood of atoms enclosed by a sphere of a radius r . For atom j , the instantaneous temperature of each atomic site can be calculated by

$$T_j = \frac{2E_j}{3k_B} \quad (6)$$

where k_B is the Boltzmann constant, and E_j is the kinetic energy of all atoms in the sphere.

The heat flux through a volume is calculated as follows [9]:

$$q = \frac{1}{2V} \left[\sum_i m_i v_i^2 v_i + \sum_i \sum_{j \neq i} \phi_{ij} v_i - \sum_i \sum_{j \neq i} (r_{ij} f_{ij}) v_i \right] \quad (7)$$

where the first and second terms related to summations of kinetic and potential energy carried by a molecule i . The third term, the tensor product of vectors r_{ij} and f_{ij} , represents the energy transfer by the pressure work. Because of the third term, the calculation of heat flux is not trivial at all. The thermal conductivity can be calculated based on the temperature gradient and heat flux as follows [9]:

$$\lambda = q / (\partial T / \partial z) \quad (8)$$

In the last few decades, various theoretical models were developed to explain thermal behavior at interfaces. For example, the acoustic mismatch model [10] and the diffuse mismatch model [11], both models were developed to describe how and why phonons are interrupted at interfaces. The diffuse mismatch model differs from the acoustic mismatch model mainly in the derivation of the transmission probability. Molecular dynamics simulations can be used as a means of investigating transport in more realistic anharmonic crystal models. It can be used to simulate interfacial thermal transport dependence on temperature for the interfaces. In this MD model, the expression of the thermal boundary resistance is given as follows [6]:

$$R_B = \frac{\pi^2 k_B^4}{15 h^3} \left(\sum_j v_{1,j}^2 \Gamma_{1,j} \right)^{-1} T^{-3} \quad (9)$$

where T is the temperature at the interface, and Γ is the transmission coefficient of the material of origin for mode of propagation j . Γ is defined as follows:

$$\Gamma_{1,j} = \int_{\theta=0}^{\pi/2} \alpha(\theta)_{1 \rightarrow 2} \cos(\theta) \sin(\theta) d\theta \quad (10)$$

where θ is the angle of incidence.

IV. Coupling Between Atomic and Finite Element Models

A. Mixed Region of MD and FE

A key issue that needs to be carefully addressed is the consistent treatment between the continuum and atomic descriptions. Assuming that FEM and MD are the two specific computational approaches being used, links need to be established to couple the two methods. Applying various boundary conditions to the atomic model is rather cumbersome. Therefore, it is beneficial to couple the atomic model with the finite element model along the boundaries of the atoms. Then boundary conditions can be disposed for the finite element model more easily. To make the discrete atoms as a continuous medium, the atomic model and the finite element model of the continuous medium must be mixed properly. A widely used approach is to implement the coupling through a so-called handshake region, which is essentially the interface between the FEM and MD regions [8,12]. For simplicity, by considering a two-dimensional coupling between the two models, the same algorithm can be applied to three-dimensional bodies. The intermediate domain is named the coupled domain, in which both atoms and finite element meshes overlap each other.

B. Temperature-Dependent Processes in FE/MD Region

In the model, the atomic temperature in the coupled region is interpolated through the FEM shape function; the interpolated atomic temperature is then used as the boundary condition for the

MD region. The method proposed by Liu and Plumbridge [15] was used to ensemble the kinetic energy in the FE region and to derive a continuum (FE) temperature equation.

In multiscale coupling, a separate energy equation is needed in the FE region. The propagation of the energy generated in the MD region as heat into the FE region is important for accurately simulating the dynamics. The ensemble average of the kinetic energy can be calculated as follows [16]:

$$\langle K \rangle = \frac{1}{2} \dot{u}^T M \dot{u} + \frac{3}{2} k_B T (N_a - n_c) \quad (11)$$

where k_B is Boltzmann constant, N_a is the number of atoms, N_c is the number of nodes in the FE region, and T is the temperature. The first term on the right-hand side is simply the coarse-scale kinetic energy, and the second term can be thought of as the contribution of temperature to internal energy: that is, the kinetic energy that is not represented by the coarse-scale (FE-region) description.

A continuum (FE) temperature equation can be deduced by using the projection operator technique [13]. The information about MD velocities and atomic masses is introduced as follows

$$\sum_j M_{IJ} T_j = \frac{1}{k_B} \sum N_I(X_n) m_n^2 \dot{q}_n^2 H_n \quad (12)$$

where the summation is performed over a discrete set of quadrature points X_n ; M_{IJ} are the components of the FE mass matrix; T is the nodal temperature matrix; and m , \dot{q} , and H are, respectively, the representative FE mass, atomic velocity, and quadrature weight associated with point X_n . At those locations, where no direct MD solution is available, the velocities can be calculated as follows [13]:

$$\dot{q}_n(t) = \int_0^t \dot{w}_n(t - \tau) q_0(\tau) d\tau \quad (13)$$

where q_0 is the displacement at the atomistic/continuum interface.

C. Solution Procedure

The atomic and finite element models are solved independently in a staggered manner. The solution procedure for the coupled problem is explained next:

- 1) Solve the finite element domain equation $[K_f]\{u_f\} = \{Q_f\}$. Subscript f denotes the finite element.
- 2) Calculate the embedded-atom temperatures based on the finite element nodal temperatures using the finite element shape functions such as $\{u_a^e\} = [N]\{u_f^e\}$. The superscripts a and e indicate, respectively, the atomic region and embedded atoms or finite elements containing such atoms, and $[N]$ is the shape function matrix of finite elements.
- 3) Obtain the new velocities of the embedded atoms according to the results of step 2 by the temperature-bath method.
- 4) Calculate the new positions $\{r_a^e\}$ of the embedded atoms.
- 5) Obtain the solution for the rest of the atoms' new positions with fixed embedded-atom positions using the atomic model.
- 6) Calculate the thermal flux $\{Q_a^e\}$ on the embedded atoms exerted by all atoms.
- 7) Calculate the equivalent nodal thermal flux of the finite elements containing the atoms by using

$$\{Q_f^e\} = \int_{V^e} [N]^T \{Q_a^e\} dV$$

where V^e is the element volume containing the embedded atoms.

- 8) By using the aforementioned results, the new finite element solution can be obtained. Then repeat the process from step 2.

V. Simulations and Analysis

A. Model Construction

The construction of the model is shown in Fig. 1. In the FE region, the temperature distribution can be governed by the following equation:

$$\rho C_p \frac{\partial T}{\partial t} - \nabla \cdot (k \nabla T) - Q = 0 \quad (14)$$

where ρ is the material density, C_p is the constant pressure specific heat, t is the time, k is the thermal conductivity, and Q is the volumetric heat source. The first term in Eq. (14) represents the energy accumulation term, the second term denotes the inlet/outlet heat-flux difference over a unit volume, and the last term defines the volumetric heat-source/sink term. Here, the uniform heat flux with density q is applied to the bottom surface of the FE region of Cu, which is the heat source. The top surface of the FE region of Al is convectively cooled and other surfaces are adiabatic. The boundary conditions in the present model are defined by using the so-called Neumann-type conditions that specify the outward heat flux, $n \cdot (k \nabla T)$, where n is the outward surface normal. At the top surface of the FE region of Al, the outer heat flux is set equal to the convective heat flux, $h(T_{\text{inf}} - T)$, where h denotes the heat transfer coefficient and T_{inf} is the temperature of the surrounding environment. No heat transfer by radiation is considered.

The MD model can be initiated by selecting Cu and Al as simulation materials and formed as a face-centered cubic structure. The total numbers of Cu and Al atoms are 13,824 and 9261, respectively. And the numbers of nodes in the FE regions for Cu and Al are 6022 and 5805, respectively. The embedded-atom method potentials and their parameters for Cu and Al can be found based on [7,14], respectively. The two dimensions in Fig. 2 are in x [1 0 0] and z [0 0 1]. The velocity-Verlet algorithm was used to march the atoms through time. The time-step size used in each simulation was 1×10^{-9} s. The cutoff distance in all cases was set as $r_c = 2.6\sigma$. Periodic boundary conditions are used except in the z direction (normal to the interface). The distance between the Cu block and Al block is initialized as the average of the characteristic length scale for Cu and Al. The coupled region is initialized as shown in Fig. 2, in which both atoms and finite element meshes overlap each other.

B. Simulation Results

The temperature distribution near the interface is shown in Fig. 3a. The average temperatures of the atomic layers are shown in Fig. 3b.

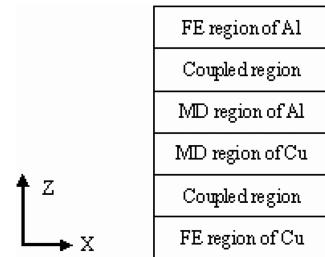


Fig. 1 Construction of the model.

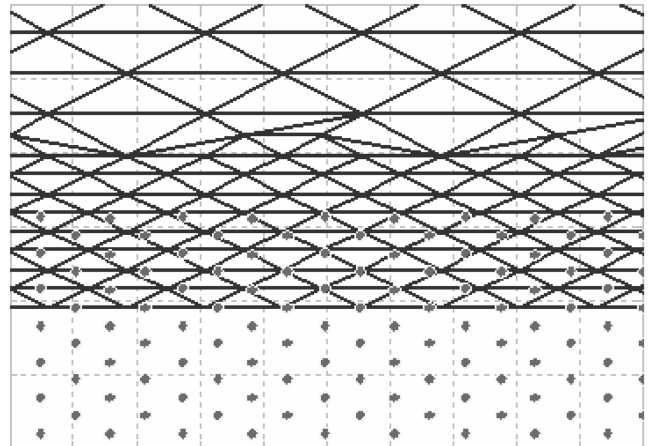
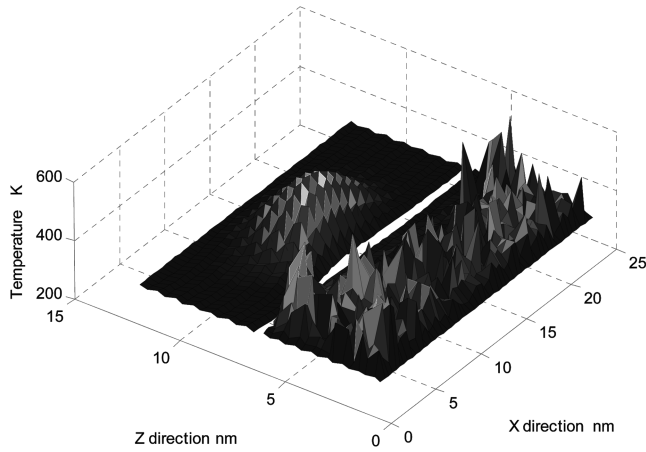
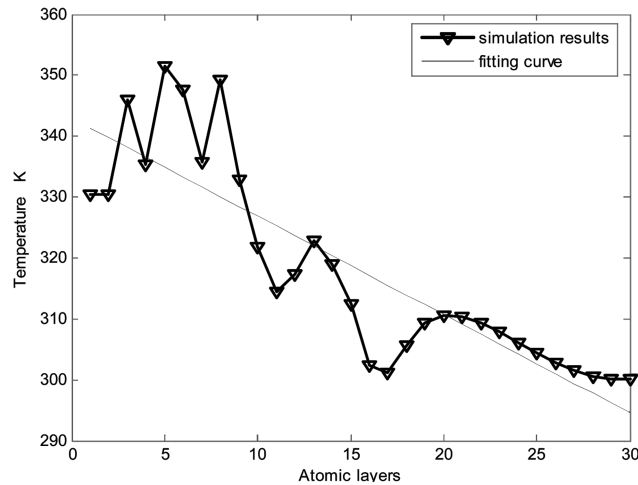


Fig. 2 Configuration of coupled region.



a) The temperature distribution near the interface



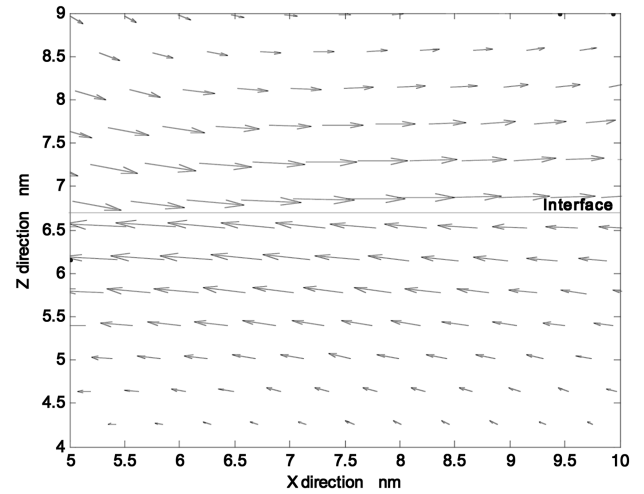
b) Average temperatures of the atomic layers near the Cu-Al interface

Fig. 3 Temperature distribution at 20,000 time steps.

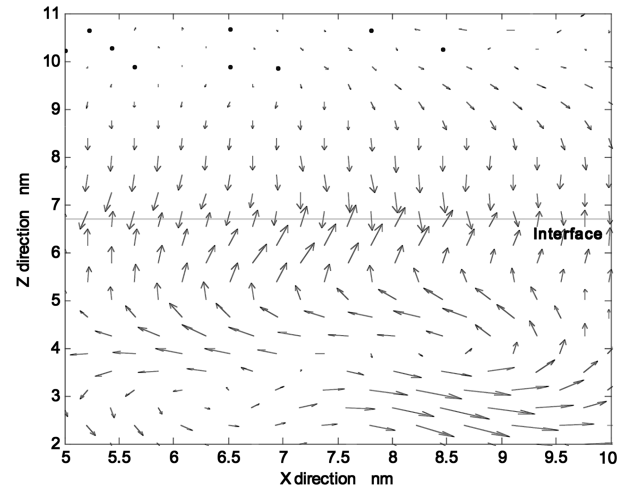
These figures show that the temperature will drop suddenly at the interface, owing to the interface thermal resistance. By the simulation results, the interesting point that is to be noted is that right at the interface, there is a jump in temperature. The interfacial temperature increases at first and then decreases severely. It means a high-temperature region exists at the interface.

Figure 4 shows the vector-field results of atom displacements. As shown in Fig. 4a, the atoms of dissimilar materials near the interface tend to move with reverse directions. The movements will generate microcracks near the interface, which may give an explanation for the crack-generation mechanics in the electronic packaging. In the meantime, two blocks of Cu are chosen to build the interface. The corresponding vector-field results of atom displacements are shown in Fig. 4b. Figure 4b shows that the atoms of dissimilar blocks tend to move toward the interface (x direction), which is different from the results shown in Fig. 4a. So it can be concluded that the characteristic of atoms moving along the interface is caused by a dissimilarity of material, which reveals the damage mechanism at the interface in heat transfer.

The heat transfer across the dissimilar-materials interface takes place through surface-asperity microcontacts and through air-filled microgaps and is hence, associated with a significant thermal resistance. A variety of materials commonly referred to as thermal interface materials have been developed. These materials are used to reduce or completely eliminate the air gaps from the contact interfaces by conforming to the rough and uneven mating surfaces. However, very few studies focus on how interatomic interactions at the interface affect thermal resistance, whereas it can be easily investigated here. As shown in Fig. 5, for a smooth interface, the thermal resistance can also be generated by interatomic interaction.



a) The atoms of dissimilar materials near the interface tend to move with reverse directions



b) The atoms of dissimilar blocks tend to move toward interface

Fig. 4 Vector field results of atom displacements.

In the primary stage, the interfacial thermal resistance is unstable and will become very large at a certain time. At the last stage, the change of interfacial thermal resistance tends to be stable. The variation of interfacial thermal resistance with time is quite similar to the experimental results obtained by Massé et al. [16].

Diffusion bonding is a solid-state welding process with coalescence of contacting surfaces. It is produced with minimum macroscopic deformation by diffusion-controlled processes, which are induced by applying heat and pressure. In this simulation, diffusion bonding exists among the interfacial atoms of different materials. The stage of thermal resistance decreasing could be considered as an unstable process in diffusion bonding. For electrically insulating materials, the macroscopic description of thermal transport originates from the diffusive dynamics of phonons that carry heat through the crystal. But for nanostructures, the characteristic of microstructural length may become comparable with the phonon mean free path. Hence, the thermal property is more likely related to the interfacial properties than to the bulk properties of the material. It should be stressed that the interfacial thermal resistance fluctuated all the time in the simulation, whereas the results from experiments [19] changed smoothly and were unable to capture the fluctuation. It is interesting that the friction force and block temperature also fluctuate all the time in nanoscale sliding [21].

VI. Conclusions

Very few studies [9,22] have addressed the issue of dissimilar-materials-interface effects on thermal properties. The issue of

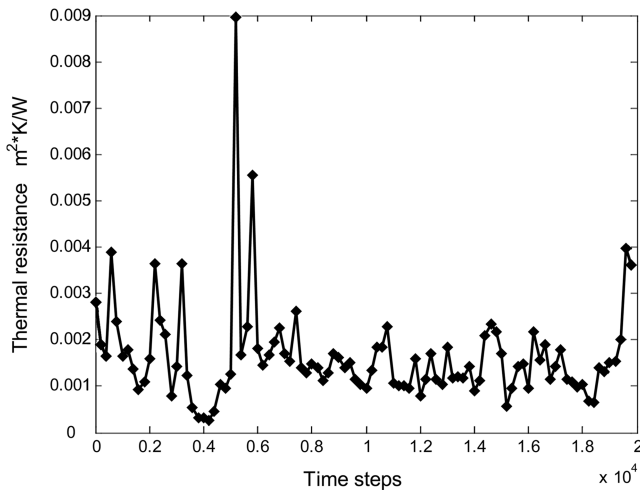


Fig. 5 Relation of interfacial thermal resistance and time steps.

determining interfacial thermal resistance by the multiscale method does not appear to have been addressed in existing literature. In this paper, a novel hybrid MD/FE simulation approach is proposed to investigate the characteristics of the Cu–Al interface during the heat transport process. An atomic model is coupled with the finite element model at the boundaries of atoms so that boundary conditions could be applied more readily to the model.

The simulations results show that the temperature distribution is nonuniform along the interface, with several places corresponding to a large temperature difference and severe plastic deformation. It means that a high-stress region exists at the interface, which will induce cracks eventually. At 20,000 time steps, with the heat transferring through the interface, the average temperature of the Al region and the temperature difference at the interface increase, and the temperature jump in the Al region is more severe. It means that the thermal stress near the interface will be raised. Moreover, the atoms of dissimilar materials move with reverse direction along the interface (x orientation), which will induce stress and voids at the interface.

By the comparative investigation, the Cu–Cu interface is built up, and the corresponding vector-field results of atom displacements and the temperature distribution are presented. It shows that the characteristic of atoms moving along the interface is caused by a dissimilarity of material, which reveals the damage mechanism at the interface in heat transfer. For thermal resistance, in the primary stage, the interfacial thermal resistance is unstable and become very large at a certain time; after 10,000 time steps, the interfacial thermal resistance tends to be stable.

The present atomic-based multiscale model is a valid approach for interfacial thermal conductance problems, and so it could be used for investigation of other interfacial behaviors of dissimilar materials.

Acknowledgments

The authors would like to acknowledge the support of the National Natural Science Foundation of China (50875115); Natural Science Foundation of Jiangsu Province of China, Innovative Foundation for Doctoral Candidate of Jiangsu Province (CX07B_069z); Special Science Foundation for Middle-Young Academic Leader of Jiangsu High Education in China (Qinglan Gongcheng Project); Natural Science Foundation for Qualified Personnel of Jiangsu University (04JDG027); and Special Natural Science Foundation for Innovative Group of Jiangsu University, Special Science Foundation for Middle-Young Academic Leader of Guangxi High Education in China during the course of this work.

References

[1] Ye H., Lin M., and Basaran, C., "Failure Modes and FEM Analysis of Power Electronic Packaging," *Finite Elements in Analysis and Design*, Vol. 38, No. 7, 2002, pp. 601–612.

doi:10.1016/S0168-874X(01)00094-4

[2] Ji, B. H., and Gao, H., "A Study of Fracture Mechanisms in Biological Nano-Composites Via the Virtual Internal Bond Model," *Materials Science and Engineering*, Vol. A366, 2004, pp. 96–103.

[3] Fan, H. B., Cell K. Y., and Yuen, M. F., "A New Method to Predict Delamination in Electronic Packages," *Electronic Components and Technology Conference*, Inst. of Electrical and Electronics Engineers, Piscataway, NJ, 2005, pp. 145–150.

[4] Liu, H. J., Wang, S. Q., Du, A., and Zhang, C. B., "Molecular Dynamics Study on Interfacial Energy and Atomic Structure of Ag/Ni and Cu/Ni Heterophase System," *Journal of Materials Science and Technology*, Vol. 20, No. 6, 2004, pp. 644–648.

[5] Johnson, R. A., "Alloy Models with the Embedded-Atom Method," *Physical Review B*, Vol. 37, No. 17, 1989, pp. 12254–12259. doi:10.1103/PhysRevB.39.12254

[6] Hegedus, P. J., and Abramson, A. R., "A Molecular Dynamics Study of Interfacial Thermal Transport in Heterogeneous Systems," *International Journal of Heat and Mass Transfer*, Vol. 49, Nos. 25–26, 2006, pp. 4921–4931. doi:10.1016/j.ijheatmasstransfer.2006.05.030

[7] Ward, D. K., Curtin, W. A., and Qi, Y., "Aluminum–Silicon Interfaces and Nanocomposites—A Molecular Dynamics Study," *Composites Science and Technology*, Vol. 66, No. 9, 2006, pp. 1151–1161. doi:10.1016/j.compscitech.2005.10.024

[8] Rudd, R. E., "Coarse-Grained Molecular Dynamics for Computer Modeling of Nanomechanical Systems," *International Journal for Numerical Methods in Engineering*, Vol. 2, No. 2, 2004, pp. 203–220

[9] Maruyama, S., "Molecular Dynamics Method for Microscale Heat Transfer," *Advances in Numerical Heat Transfer*, Vol. 2, No. 6, 2000, pp. 189–226.

[10] Khalatnikov, I. M., and Adamenko, I. N., "Theory of the Kapitza Temperature Discontinuity at a Solid Body–Liquid Helium Boundary," *Soviet Physics, JETP*, Vol. 36, No. 3, 1973.

[11] Swartz, E. T., and Pohl, R. O., "Thermal Resistance at Interfaces," *Applied Physics Letters* Vol. 51, No. 26, 1987, pp. 2200–2202. doi:10.1063/1.98939

[12] Qian, D., Wagner, G. J., and Liu, W. K., "A Multiscale Projection Method for the Analysis of Carbon Nanotubes," *Computer Methods in Applied Mechanics and Engineering*, Vol. 193, Nos. 17–20, 2004, pp. 1603–1632. doi:10.1016/j.cma.2003.12.016

[13] Liu, W. K., Karpov, E. G., Zhang, S., and Park, H. S., "An Introduction to Computational Nanomechanics and Materials," *Computer Methods in Applied Mechanics and Engineering*, Vol. 193, Nos. 17–20, 2004, pp. 1529–1578. doi:10.1016/j.cma.2003.12.008

[14] Mei, J., Davenport J. W., and Fernando G. W., *Phys. Rev. B*, Vol. 43, No. 6, 1991, pp. 4653.

[15] Liu, X. W., and Plumbbridge, W. J., "Thermomechanical Fatigue of Sn–37 wt.% Pb Model Solder Joints," *Materials Science and Engineering A*, Vol. 362, Nos. 1–2, 2003, pp. 309–321. doi:10.1016/S0921-5093(03)00638-5

[16] Massé, H., Arquis, É., Delaunay, D., and Quilliet, S., "Heat Transfer with Mechanically Driven Thermal Contact Resistance at the Polymer–Mold Interface in Injection Molding of Polymers," *International Journal of Heat and Mass Transfer*, Vol. 47, Nos. 8–9, 2004, pp. 2015–2027. doi:10.1016/j.ijheatmasstransfer.2002.04.001

[17] Kelkar, M., Phelan, P. E., and Gu, B., "Thermal Boundary Resistance for Thin-Film High-TC Superconductors at Varying Interfacial Temperature Drops," *International Journal of Heat and Mass Transfer*, Vol. 40, No. 11, 1997, pp. 2637–2645. doi:10.1016/S0017-9310(96)00279-7

[18] Ping, Y., Ningbo, L., Daoguo, Y., and Ernst, L. J., "Sliding Simulation for Adhesion Problems in Micro Gear Trains Based on an Atomistic Simplified Model," *Microsystem Technologies*, Vol. 12, No. 12, 2006, pp. 1125–1131. doi:10.1007/s00542-006-0235-7

[19] Abramson, A. R., Tien, C. L., and Majumdar, A., "Interface and Strain Effects on the Thermal Conductivity of Heterostructures: A Molecular Dynamics Study," *Journal of Heat Transfer*, Vol. 124, No. 5, 2002, pp. 963–970. doi:10.1115/1.1495516

[20] Ping, Y., Ningbo, L., and Daoguo, Y., "Property Simulation for Nano-Scale Interfacial Friction Between Two kinds of Material in MEMS Based on an Atomistic Simplified Model," *International Journal of Modern Physics B*, Vol. 21, No. 20, 2007, pp. 3581–3590. doi:10.1142/S0217979207037582

[21] Ningbo, L., and Ping, Y., "Effect of Temperature on Nano-Scale

Adhesion for MEMS,” *International Journal of Materials and Product Technology*, Vol. 31, Nos. 2–4, 2008, pp. 354–364.
doi:10.1504/IJMPT.2008.018032

[22] Ping Y., and Huazhong Z., “Numerical Analysis on Meshing Friction Characteristics of Nano-Gear Train,” *Tribology International*, Vol. 4, No. 6, 2008, pp. 535–541